A Novel Deceleration Concept Based on Modulating Lift-to-Drag through Actuating the Payload Mass

State University of New York at Buffalo, Buffalo, New York 14260

Technical Paper
Advisor: Dr. Kemper Lewis
Due Date: March 5, 2015

Henry Kwan
Levi Li
Samuel Tedesco
Anibal Martinez

Table of Contents

ABSTRACT: NASA is actively developing the technologies and capabilities required to send humans to Mars in the 2030s. The use of Hypersonic Inflatable Aerodynamic Decelerator (HIAD) technology is critical to the next engineering design of hypersonic entry vehicles. Currently NASA seeks novel and robust ideas and applications for generating lift using HIAD technology. In order to better understand the problem, a systems analysis is done on the requirements which resulted in a Technical Readiness Level (TRL) of the project. The proposed concept of a payload shifting mechanism is described in detail which discusses the components and how the mechanism works: power, automation, and material. The mechanism is further analyzed with technical information through Finite Element Analysis (FEA) to determine the levels of stress & areas of stress concentrations, and also through calculations on the effect of the mechanism on modulating the Lift-to-Drag (L/D). The FEA also provides a significant amount of information on the material choice which ultimately has a significant effect on the weight; this is also an important factor in the design of the mechanism. A cost analysis is also calculated to determine the overall projected cost of building the mechanism. The paper ends with a discussion of the project plan & schedule which describes the future steps necessary in order to take advantage of the concept proposed.

NOMENCLATURE

α	angle of attack	M_1	mach initial
A	area	M_2	mach final
C_D	coefficient of drag	M_{n1}	mach upstream
C_L	coefficient of lift	M_{n2}	mach downstream
θ	conical angle	a, b, c, λ, X	mach wave angle relations
ρ	density	β	mach wave angle
D	drag	γ	specific heat ratio
v	fluid kinematic viscosity	P	pressure
g	gravitational acceleration	Re	Reynolds number
h	height of TPS	T	temperature
H	altitude	T_m	molecular-scale temperature
L	lift	u	velocity
M	mach number		

I. Objective

Our objective is to design and analyze a system to create a 0.2 - 0.5 Lift-to-Drag (L/D), and to be able to vary the L/D in a short amount of time during entry into the Martian atmosphere. To accomplish this, a design of a mechanism to modulate the L/D was created which was virtually prototyped and tested with 3D Computer Aided Design (CAD) modeling and Finite Element Analysis (FEA).

II. Systems Analysis of Requirements

II.I Engineering Requirements

In our identification of stakeholder requirements, we developed a comprehensive set of engineering specifications. Using interrelationship matrices, we then determined the five most important specifications which are shown in Table I. These specifications will become the key criteria for the success of our design.

These specifications were also used to analyze and evaluate our different concept alternatives, resulting in a concept that we felt best satisfied our engineering specifications and stakeholder requirements.

Table 1: Analysis of Engineering Requirements

Rank	Engineering Requirement	Benchmark
1.	Time required to vary lift-to-drag ratio over full range	Minimal
2.	Total system mass	Low
3.	Shape of outer mold line (design simplicity)	Smooth
4.	Complexity of system	Minimal
5.	Total system cost	Low

We evaluated the interrelationship between our full set of engineering requirements in order to better predict the critical interfaces and to understand the tradespace we will be navigating in our final design. Understanding these tradeoffs allowed to use to develop a set of innovative design options from which to determine our final concept and its technical readiness level.

II.II Technical Readiness Level

From developing our detailed Computer Aided Design (CAD) model and preparing system simulations based on Finite Element Analysis (FEA), the technical readiness level of our final concept will be at TRL 3. Given the feasibility of our concept and the expertise we have in our project team and advisory faculty, a strong foundation will exist to take to TRL levels 4 - 6.

III. PROPOSED CONCEPT

One of the original proposals made by our team was a tubular structure for the HIAD, as shown in Figure 1. The idea behind that it was that it might be possible to decrease the weight of the HIAD without significantly affecting the structural integrity of the HIAD at least when compared to the current axisymmetric design of the HIAD structure. Since the submission of the white paper, our team has come to the conclusion that the effort and time needed to implement a redesign of the HIAD structure would not be beneficial to this project, along with avoiding the hotspots that might cause problems with the tubular structure design. The main focus of the remainder of this section is the design of the payload shift mechanism.

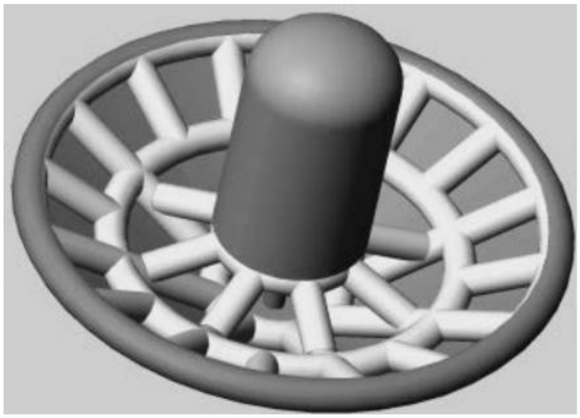

Figure 1: Tubular Structure Proposed in White Paper

The proposed concept leverages the enormous amount of weight from the payload. In order to modulate the L/D, the payload will be shifted and thus shift the center of gravity of the entire system. This will be done through a payload shift mechanism which incorporates a series of actuators to position the payload. The mechanism can be altered quickly and without much delay, which will allow the Lift/Drag ratio to be modulated through its whole range instantaneously. The actuator system would consist of three actuators installed on a circular brace each separated by 120°. Each of these actuators would be supplemented by two smaller actuators that are attached to the circular brace and to the base of the larger actuator. This would allow the actuator system to have two degrees of freedom, which should be enough to alter the location of the payload and in turn change the location of the center of gravity in order to exercise control over the Lift/Drag ratio. This system should have the capability to quickly modulate the HIAD through the whole range of its Lift/Drag ratio. An overview of the entire system with the payload shift mechanism is shown in Figure 2.

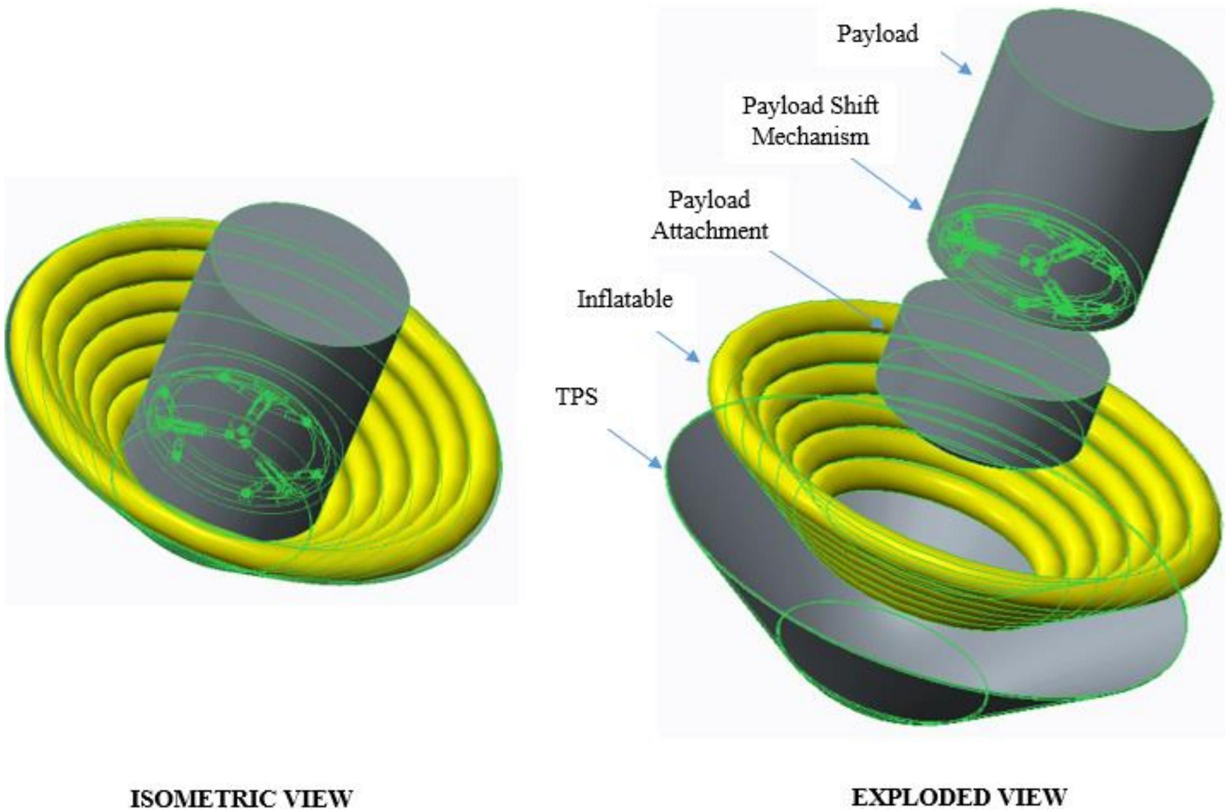

Figure 2: Isometric & Exploded View of the Entire System

There are three large actuators that are assisted through six small actuators. This can be seen in Figure 3. Hydraulic actuators should provide a quick response time, which should enable the payload shift mechanism to quickly move the payload in order to change the location of the center of gravity. Hydraulic actuators would provide a suitable response time so that the L/D can be modulated throughout its entire range within a few seconds. A potential disadvantage to using a hydraulic actuator would be the addition of hoses and lines that would be needed in order to deliver the fluid from the pump to the actuators and back, including the potential for leakage which would negatively affect the performance of the hydraulic system. We feel that this disadvantage would be significantly outweighed by the benefits of the hydraulic system which would help the payload shifting mechanism to effectively and rapidly modulate the Lift/Drag ratio of the HIAD in order to help it slow down to a suitable landing speed. This system should also have the ability to hold a specific L/D during flight in order to enable the HIAD to control its trajectory and allow it to land in a specific location.

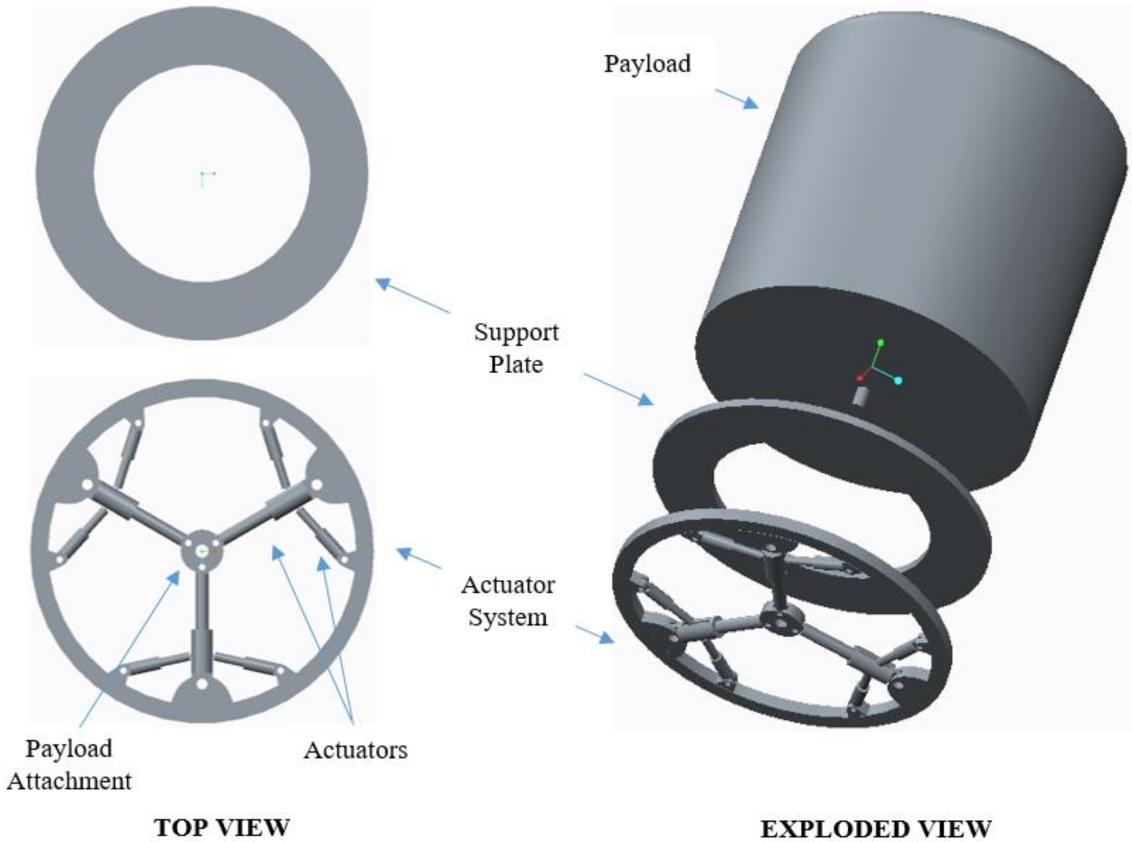

Figure 3: Top & Exploded View of the Top Payload Structure with Payload Shift Mechanism

The hydraulic actuators for this system would need to be customized for this application in order to ensure the mechanism works properly. Current commercially available industrial actuators have the ability to support loads up to 20 tons and have a stroke length of four to six inches. Through analysis, our team has estimated that a stroke length of about 15 - 20 inches, illustrated in Figure 4, would be needed in order to provide the greatest amount of control in modulating the L/D as the location of the center of gravity is changed and also allow for small adjustments which would give the HIAD a greater amount of control of its trajectory and target destination. Since the actuators would all be custom made, the optimum number of pumps required to make sure the system works as intended would need to be determined; based on the fluid they will need to compress in order to provide the appropriate amount of force to move the payload. This optimization will also need to minimize the system response time while determining the correct stroke length required. Specific information for the mechanism include the following:

- **Power**: The actuators would be powered by electric pumps that can deliver an appropriate amount of pressure. The pumps need to be able to provide the required force and pressure to the actuators when needed. They should also be able to sustain the required pressure for extended periods of time in cases where the payload needs to be shifted to a specific location in order to maintain a specific value of the Lift/Drag ratio. It would also be required to make sure that the entire hydraulic system is properly insulated so that each component can work at its optimal temperature, this can help ensure that the entire payload shifting mechanism works as intended. Going forward the amount of hydraulic fluid needed and the pressure that the pumps needs to provide will need to be determined in future analyses in order to make sure that the payload shifting mechanism works as intended.

- **Automation**: The entire payload shift mechanism will be completely automated. Sensors will be placed throughout the interior of the HIAD that will interact with an onboard computer system. The sensors that will be used include 3-axis accelerometers and ultrasonic rangefinders. The 3-axis accelerometer will give information on the current orientation of the HIAD as it enters the Martian atmosphere, and this information will be sent to the onboard computer. The onboard computer will then control the payload shift mechanism and simultaneously move all nine actuators. The ultrasonic rangefinders will be placed along the payload and will give the computer more information on how far the payload has shifted.
- **Material**: The current material selection for the construction of the entire mechanism is steel. Steel is used based on the weight of the payload. A more in depth materials analysis is shown in Section III.I where a Finite Element Analysis (FEA) is performed to demonstrate the stress concentrations of the mechanism and the effect of the material selection has on the stresses throughout the mechanism. However, through the FEA, it was also shown determined that a tungsten support plate would create reduce the stress.

IV. ANALYSIS

This section includes an FEA done on the payload shift mechanism for the payload centered & shifted, as well as for different materials. The calculations shown, demonstrate the modulated L/D requirements and the shift in center of gravity as a function of the payload.

IV.I Finite Element Analysis

In order to create the most optimal design of the payload shift mechanism, the team leveraged FEA and CAD in order to determine where most of the stress concentrations would occur and what the maximum stress would be at these concentrations. Through these analyses, the team made several design changes in order to minimize material and eliminate stress concentrations. FEA was used in order to simulate the Von Mises Stress, Principle Stresses, Maximum Shear Stress, Displacement Magnitude, and Principle Stress Vectors. In our analysis, it was determined that the Von Mises Stress would be more accurate and therefore the Principle and Maximum Shear Stresses are not shown. All stresses are in MPa.

IV.I.I Payload Shift Mechanism Centered

In order to optimize the design of the mechanism, an FEA was first performed on the system with the payload centered or not shifted. By doing so, we learned a significant amount about the original design including the fact that the; most stress concentrations occurred where surfaces were perpendicular to one another or essentially sharp edges. Therefore, to remove these concentrations, round edges were added to the parts which greatly reduced the maximum stress on the mechanism.

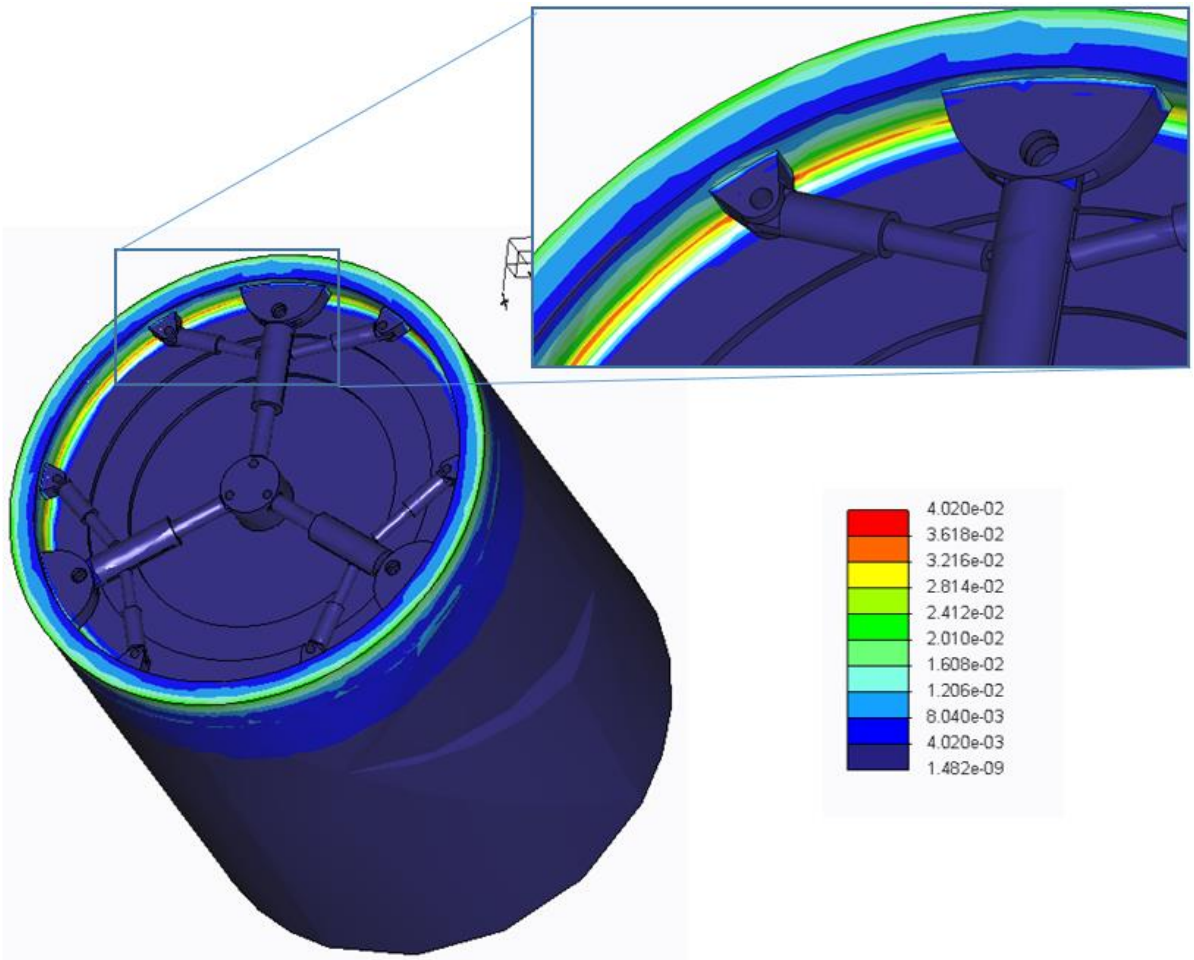

Figure 4: Stress Von Mises [MPa], Payload Centered

Figure 5 illustrates an analysis that was done on the mechanism after the design change was made. As shown in the enlarged view, the stress concentrations still occur at the round edge, however, the maximum stress that occurs is $4.020 \cdot 10^{-2}$ MPa. This was significantly reduced from the original design. The material used for this analysis was steel since when we used Aluminum, the stress significantly increased. Aluminum would reduce the mass of the system which is important. However, to ensure the strength and rigidity of the system, steel was determined to be the optimal material.

IV.I.II Payload Shift Mechanism Shifted (Steel vs. Tungsten Support Plate)

The mechanism was also analyzed with the payload shifted, as shown in Figure 6. From initial analysis, it was determined that most of the force from the payload was applied on the support plate. Therefore, two separate analyses were conducted with the payload shifted; one with a steel support plate and the other with a tungsten support plate. Tungsten was chosen because it has better material properties than steel such as durability and strength.

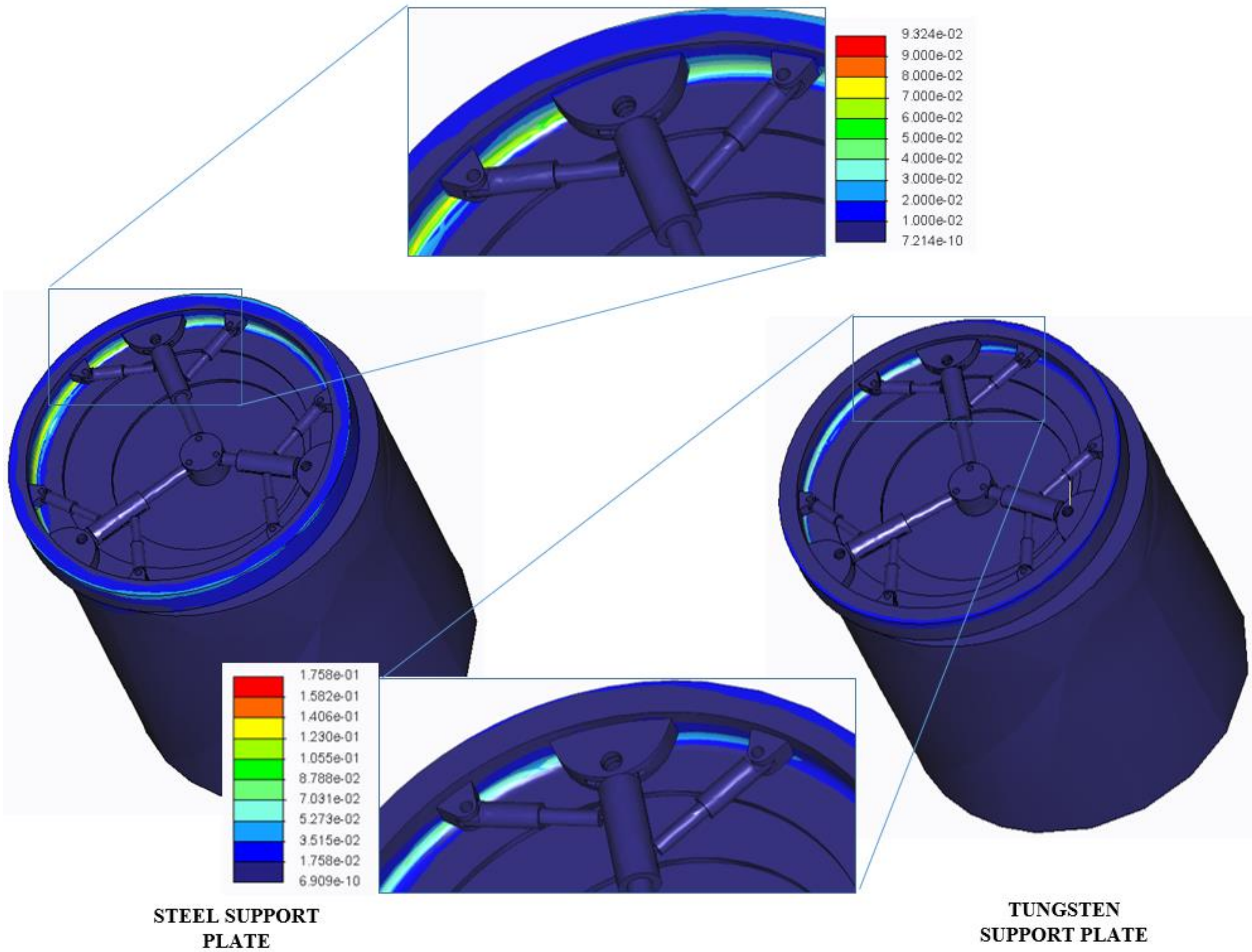

Figure 5: Von Mises Stress [MPa], Payload Shifted (Steel vs. Tungsten)

Illustrated in Figure 5, the analysis with the steel support plate on the left, and the analysis with the tungsten material on the right. From the enlarged view, it can be seen that there is a significant reduction in the magnitude of the stress from steel to tungsten. The maximum stress with the steel support plate is $8.0 \cdot 10^{-2}$ MPa and $5.273 \cdot 10^{-2}$ MPa for tungsten. Therefore, a different material such as tungsten should be considered for the final design.

IV.I.III Displacement Magnitudes & Principle Stress Vectors

Figure 7 shows the displacement magnitudes and principle stresses of the shifted and non-shifted payload, with a tungsten support plate. The displacement at the outside of the payload shifting mechanism without shift is zero, and increases radially inward. Subsequent testing will be done to make sure the payload attachment can withstand this magnitude, with the option of reinforcement in mind. For the shifted payload, the greatest magnitude is seen on the support plate. The actuators of the non-shifted mechanism hold little to no principle stresses, with the exception of their joints. The outside of the support ring holds a fair amount of compression, which can be reduced with further reinforcement. The principle stresses of the shifted payload are seen in the bottom right part of the figure. Once again, there are little to no principle stresses in the actuators. Most of the stress is seen at the interface of the support ring and the outside of the actuator system. Reinforcement will be implemented as necessary.

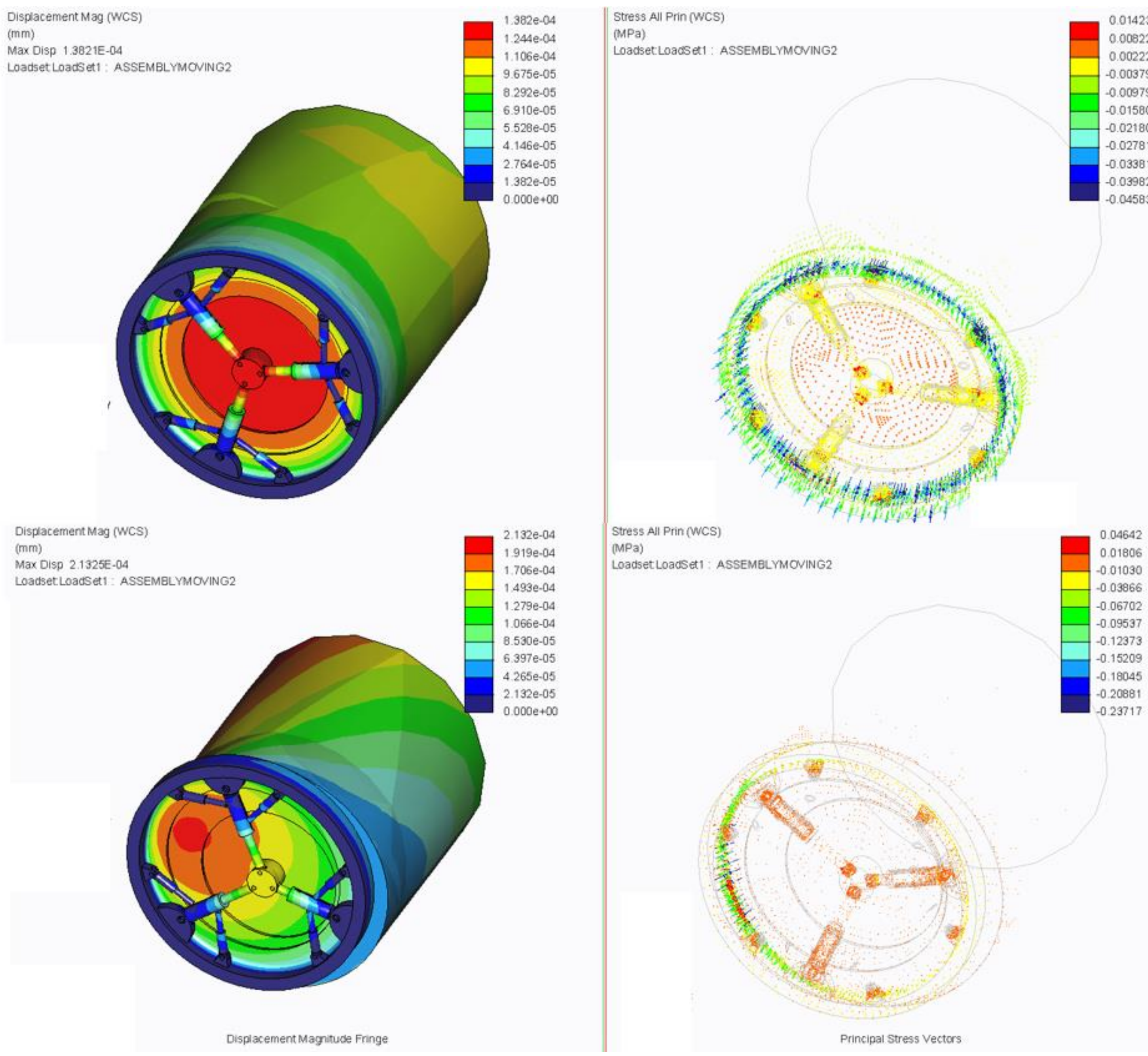

Figure 6: Displacement Magnitudes & Principle Stress Vectors [MPa], (Centered and Tungsten-Shifted)

IV.II Calculations

The main calculations performed to calculate the shift in center of gravity due to the payload mass and the modulated L/D through the Mars entry are shown in this section.

IV.II.I Shift in Center of Gravity

Given a payload mass of 15-30 metric tons, it can be assumed that most of the mass of the entire system is from the payload and the payload shifting mechanism. To calculate the shift of center of gravity:

Given:

- Payload Mass, $m_{payload}$ = 30,000 kg (30 tons)
- Payload Shifting Mechanism, $m_{mechanism}$ = 2,360 kg

Prevalent Assumptions:

- Axially symmetric structure along the y-direction
- The center of gravity is shifted along the xz plane
- Mass from TPS and Inflatable Structure are negligible

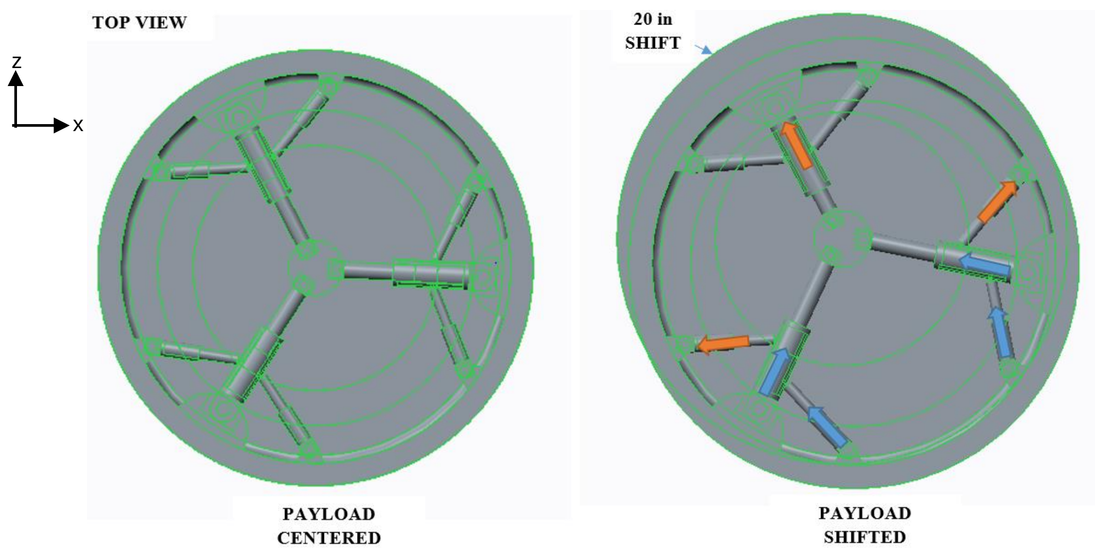

Figure 7: Top View of the Payload Centered & Shifted

The center of gravity will only be shifted in the XZ plane and therefore, with the use of CAD software, as shown in Figure 7, the shift in payload mass is 20 in. Also shown in Figure 7, is the movement of the actuators when the payload is shifted.

Eq. 1

$$x_{shift,max} = \frac{m_{payload}x_{payload} + m_{mechanism}x_{mechanism}}{m_{payload} + m_{mechanism}} = \frac{30{,}000\ kg(20\ in) + 2{,}360\ kg(0\ in)}{30{,}000\ kg + 2{,}360\ kg}$$

$$x_{shift,max} = 18.5\ in$$

IV.II.II Modulated Lift-to-Drag

Using data collected and referenced from NASA's HIAD resources, Mach number is given to be 10.2 at the height of 50 km. The angle attack generated by the payload shifting mechanism for this calculation is 25°.

Given:

- $M = 10.2$
- $\gamma = 1.28$
- $\theta = 25°$
- $\alpha = 30°$

Prevalent Assumptions:

- Atmosphere of Mars is calorically perfect
- HIAD TPS is conical shaped
- Angle from a point on the edge of TPS to the base of TPS is 50°
- Bernoulli's principles apply
- Sunny day in Mars at 20°N

On the assumption of a conical shape, it allows the HIAD to have two connected points on its base. Calculations to find lift, drag, and lift-drag ratio were then conducted by analyzing the oblique shocks generated by the hypersonic entry. The specific heat ratio is calculated at certain geopotential altitudes:

Eq. 2

$$\gamma = 0.000001409{T_m}^2 - 0.001192T_m + 1.5175$$

Where T_m = molecular-scale temperature. T_m is a function of the geopotential altitude and since the altitude is 50 km, the corresponding equation for T_m is:

Eq. 3

$$T_m = 271.1 - 2.35h = 271.1 - 2.35\ (50\ km) \qquad T_m = 153.6\ K$$

Thus the specific heat ratio on mars can be approximated:

Eq. 2, T_m

$$\gamma = 0.000001409(153.6\ K)^2 - 0.001192(153.6\ K) + 1.5175 \qquad \gamma = 1.37$$

To find the pressure at the oblique shock, the Mach wave angle must be calculated. It is found by using the Mach wave angle relations a, b, c, λ and X; Equations 3 – 7:

Eq. 4

$$a = \left[1 + \frac{\gamma - 1}{2}{M_1}^2\right]\tan(\theta) = \left[1 + \frac{1.37 - 1}{2}(10.2)^2\right]\tan(25°) \qquad a = 9.4415$$

Eq. 5

$$b = \left(1 - M_1{}^2\right) = (1 - 10.2^2) \qquad b = -103.04$$

Eq. 6

$$c = \left[1 + \frac{\gamma + 1}{2} M_1{}^2\right] \tan(\theta) = \left[1 + \frac{1.37 + 1}{2}(10.2)^2\right] \tan(25°) \qquad c = 57.9562$$

Eq. 7

$$\lambda = \sqrt{b^2 - 3ac} = \sqrt{(-103.04)^2 - 3(9.4415)(57.9562)} \qquad \lambda = 94.74$$

Eq. 8

$$X = \frac{9abc - 2b^3 - 27a^2}{2\lambda^3} = \frac{9(9.44)(-103.04)(57.96) - 2(-103.04)^3 - 27(9.44)^2}{2(94.74)^3} \qquad X = 0.9867$$

n = 2 is used for a weak shock solution.

Eq. 9

$$\beta = tan^{-1}\left(\frac{-b + 2(\lambda)(cos\left[\frac{\text{acos}(X)}{3} + \frac{2\pi n}{3}\right]}{3a}\right) = tan^{-1}\left(\frac{-103 + 2(94.74)cos\left[\frac{\text{acos}(0.9867)}{3} + \frac{2\pi(2)}{3}\right]}{3(9.44)}\right) \qquad \beta = 30.98°$$

Now that beta is found, Mach number properties of an oblique shock can be found:

Eq. 10

$$M_{n1} = M_1 \sin(\beta) = 10.2(\sin(30.98)) \qquad M_{n1} = 5.2505$$

Eq. 11

$$M_{n2} = \sqrt{\frac{1 + \frac{(\gamma - 1)}{2} M_{n1}{}^2}{\gamma M_{n1}{}^2 - \frac{(\gamma - 1)}{2}}} = \sqrt{\frac{1 + \frac{(1.37 - 1)}{2}(5.644)^2}{1.37(5.25)^2 - \frac{(1.37 - 1)}{2}}} \qquad M_{n2} = 0.4029$$

Eq. 12

$$M_2 = \frac{M_{n2}}{\sin(\beta - \theta)} = \frac{0.403}{\sin(30.98° - 25.0°)} \qquad M_2 = 3.8664$$

With the Mach number properties found, pressure relations can be used for the calorically perfect atmosphere. P_1 is provided to be 25 Pa at 50 km by the NASA resources so now P_2 can be found.

Eq. 13

$$\frac{P_2}{P_1} = 1 + \frac{2\gamma}{(\gamma + 1)}\left(M_{n1}{}^2 - 1\right) = 1 + \frac{2(1.37)}{(1 + 1.37)}((5.25)^2 - 1) \qquad \frac{P_2}{P_1} = 30.71$$

Eq. 14

$$P_2 = 30.7P_1 = 30.7(25.0\ Pa) \qquad P_2 = 792.88\ Pa$$

Force applied on the HIAD is directly related to the pressure applied and the angle of attack:

Eq. 15

$$F_{HIAD} = P_2 A = 792.88\ Pa(\pi(10\ m)^2) \qquad F_{HIAD} = 248{,}970\ N$$

Eq. 16

$$L = F_{HIAD}\sin(\alpha) = 279{,}804\ N(\sin(30°)) \qquad L = 105{,}220\ N$$

Eq. 17

$$D = F_{HIAD}\cos(\alpha) = 279{,}804\ N(\cos(30°)) \qquad D = 225{,}640\ N$$

Eq. 18

$$\frac{L}{D} = \frac{105{,}220\ N}{225{,}640\ N} \qquad \frac{L}{D} = 0.4663$$

On the assumption that oblique shocks are not applicable due to high stress concentrations, a normal shock can be used as well. It is assumed that the normal shock takes shape of the TPS.

Eq. 19

$$P_2 = P_\infty\left(\frac{2\gamma}{(\gamma+1)}M_\infty{}^2 - \frac{(\gamma-1)}{(\gamma+1)}\right) = 25\left(\frac{2(1.37)}{(1.37+1)}10.2^2 - \frac{(1.37-1)}{(1.37+1)}\right) \qquad P_2 = 3003.16\ Pa$$

Eq. 20

$$P_{0,2} = P_2\left[\frac{\frac{(\gamma+1)}{2}M_\infty{}^2}{\frac{2\gamma}{(\gamma+1)}M_\infty{}^2 - \frac{(\gamma-1)}{(\gamma+1)}}\right]^{\frac{\gamma}{\gamma-1}} = 3003.16\left[\frac{\frac{(1.37+1)}{2}10.2^2}{\frac{2*1.37}{(1.37+1)}10.2^2 - \frac{(1.37-1)}{(1.37+1)}}\right]^{\frac{1.37}{1.37-1}} \qquad P_{0,2} = 3234.41Pa$$

Now that pitot pressure is found, Force on the area of the HIAD can be calculated:

Eq. 21

$$F = \int P * \Delta dS$$

Where S is the surface area of the HIAD. Force is now broken up into lift and drag components. Because it is a normal shock, calculations have to be normalized to take into account the angle shifted by the payload shifting mechanism. h is the height of the TPS:

Eq. 22

$$L = \int P * \frac{(\Delta \cdot \widehat{j})}{|\Delta \cdot \hat{j}|}dS = \int 3234.41(0.423\hat{j})\ dS = 3234.41(0.4226)(\pi)\left(\frac{L}{2}\right)\left(\frac{L}{2}\right) + \sqrt{h^2 + \left(\frac{L}{2}\right)^2} \cdot \hat{j} \qquad L = 939{,}887.1\ N$$

Eq. 23

$$D = \int P * \frac{(\Delta \cdot \hat{\imath})}{|\Delta \cdot \hat{\imath}|} dS$$

$$= \int 3234.41(0.906\hat{\imath})\, dS$$

$$= 3234.41(0.906)(\pi)\left(\frac{L}{2}\right)\left(\frac{L}{2}\right) + \sqrt{h^2 + \left(\frac{L}{2}\right)^2} \cdot \hat{\imath}$$

$$D = 2{,}014{,}998.6\ N$$

Eq. 24

$$\frac{L}{D} = \frac{939{,}887.1\ N}{2{,}014{,}998.6\ N}$$

$$\frac{L}{D} = 0.4663$$

With both methods producing the same L/D, our team used calculated the results of the L/D as the system descends through Mars. The L/D was calculated from 50 to 30 km since these altitudes are where the HIAD's function of deceleration are most critical. As shown in Table 1, the Mach Number and Angle of Attack are also noted. It can be seen that as the HIAD approaches 30 km, the Mach Number exponentially decreases and the angle of attack decreases. The results are plotted in Figure 7:

Table 2: L/D During Descent

Height (km)	Mach Number	Angle of Attack	L/D
50	10.2	25°	***0.4663***
45	6.5	22°	***0.4040***
40	3.0	19°	***0.3443***
35	1.5	17°	***0.3057***
30	0.7	15°	***0.2679***

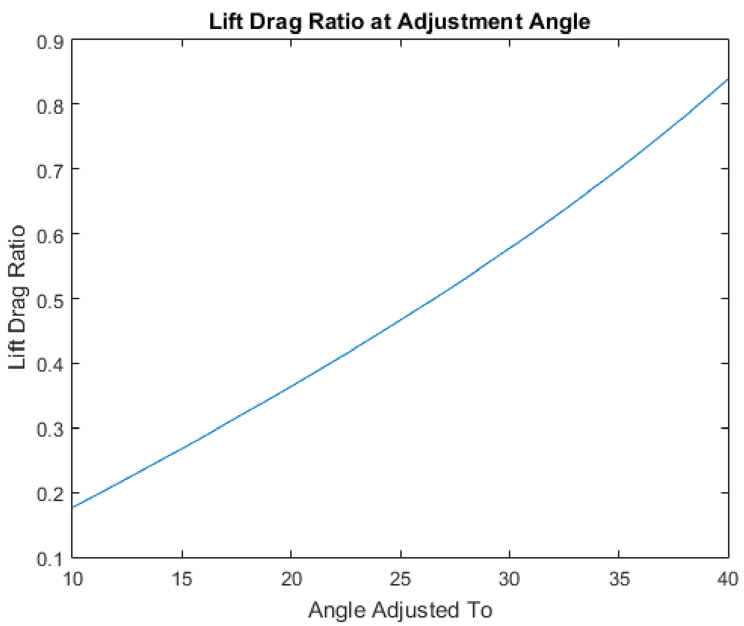

Figure 8: L/D During Descent

V. DISCUSSION

V.I Cost

The cost of the actuators was determined by scaling the cost of actuators with smaller rated loads. The large actuator should support a load of 20,000 lb., the small actuator should support a load of 10,000 lb. The cost of the support plate and outer ring were determined by calculating the volume of the parts through the CAD model and comparing it with the cost for raw material by weight. The machining costs are included to account for the manufacturing of the support plate, outer ring, and assembling the entire payload shift mechanism. As shown in Table 2, the total cost of the entire payload shift mechanism is estimated to be $213,244.50.

Table 3: Projected Costs

Part No.	Part/Method	Type	Unit Price	Quantity	Total Cost
1	Large Actuator	Steel/Chrome Plated	$1,500/unit	3	$4,500.00
2	Small Actuator	Steel/Chrome Plated	$1,500/unit	6	$9,000.00
3	Support Plate	Tungsten	$110.50/kg.	1,770 kg.	$195,585.00
4	Outer Ring	Steel	$0.05/kg.	590 kg	$29.50
5	Welding	Manufacturing Process	$3.25/ft.	40.0 ft.	$130.00
6	Plasma Cutting	Manufacturing Process	$8.33/ft. or $100/hr.	20 hr.	$2,000.00
7	Water Jet Cutting	Manufacturing Process	$8.33/ft. or $100/hr.	20 hr.	$2,000.00
				Total Cost:	**$213,244.50**

V.II Project Plan & Schedule

The outline of the project schedule for completing the design challenge is shown in Figure 9. This schedule allowed the team to reach the goal of covering all the technical aspects of the proposed concept which included an accurate and precise Computer-Aided Design (CAD) model, and FEA of the structure. If accepted, next steps of this project will take will include an oral presentation at NASA Langley Research Center. If this design were to be approved, the next stage in the process would be prototyping and testing the design of the payload shifting mechanism. Since weight and reliability are two main factors in the design of the mechanism, many different materials should be tested for the support plate where most of the stress occurs.

NASA HIAD Challenge

State University of New York at Buffalo

Today's Date: 3/5/2016 (vertical red line)

Project Lead: Henry Kwan

Start Date: 8/31/2015 Monday

First Day of Week (Mon=2):

WBS	Tasks	Start	End	Duration (Days)	% Complete	Working Days	Days Complete	Days Remaining
1	**White Paper**	9/4/15	11/14/15	72	100%	51	72	0
1.1	Discuss Project Scope	9/4/15	9/10/15	7	100%	5	7	0
1.2	Research Different HIAD Ideas	9/10/15	9/16/15	7	100%	5	7	0
1.2.1	Research HADs	9/15/15	9/19/15	5	100%	4	5	0
1.2.2	Analyze Problem	9/20/15	9/22/15	3	100%	2	3	0
1.4	Current Devices	9/20/15	9/24/15	5	100%	4	5	0
1.4.1	Generate Product List of Similar Devices	9/25/15	10/8/15	14	100%	10	14	0
1.5	Submit Notice of Intent	10/8/15	10/8/15	1	100%	1	1	0
1.6	Create differetn concepts	10/8/15	10/20/15	13	100%	9	13	0
1.6.1	Screen concepts	10/20/15	10/22/15	3	100%	3	3	0
1.6.2	Score concepts	10/20/15	10/22/15	3	100%	3	3	0
1.6.3	Analyze top concepts	10/22/15	10/24/15	3	100%	2	3	0
1.7	Choose final concept	10/25/15	10/31/15	7	100%	5	7	0
1.8	Generate White Paper	11/1/15	11/10/15	10	100%	7	10	0
1.8.1	Finalize White Paper and Submit	11/10/15	11/14/15	5	100%	4	5	0
2	**Technical Paper**	11/30/15	3/5/16	97	100%	70	97	0
2.1	Review White Paper Submission	11/30/15	12/2/15	3	100%	3	3	0
2.2	Create Embodiment Design	12/2/15	12/4/15	3	100%	3	3	0
2.2.1	Select choice of components	12/5/15	12/10/15	6	100%	4	6	0
2.2.2	Select Component Interfaces	12/10/15	12/15/15	6	100%	4	6	0
2.2.3	Select Material	12/15/15	12/20/15	6	100%	4	6	0
2.2.4	Create Geometry (dimension/shape)	12/30/15	1/15/16	17	100%	13	17	0
2.2.5	Select surface finish, fasteners/connectors	1/15/16	1/20/16	6	100%	4	6	0
2.2.6	Describe Manufacturing/Assembly Process	1/20/16	1/25/16	6	100%	4	6	0
2.3	Create Detailed Design (CAD)	1/25/16	1/25/16	1	100%	1	1	0
2.3.1	Create 3D CAD Model of Crutch Redesign	1/25/16	2/15/16	22	100%	16	22	0
2.3.2	Generate 2D View of each component	2/15/16	2/24/16	10	100%	8	10	0
2.3.3	Perform FEA and CFD analysis	2/15/16	2/25/16	11	100%	9	11	0
2.4	Generate a Bill of Materials (BOM)	2/20/16	2/24/16	5	100%	3	5	0
2.5	Generate Technical Paper	2/25/16	2/29/16	5	100%	3	5	0
2.5.1	Finalize Technical Paper and submit to NASA	3/1/16	3/5/16	5	100%	4	5	0

Figure 9: Project Schedule

VI. CONCLUSION

HIAD technology is a solution to the problem of sending large payloads Mars. This technology has the ability to increase the amount of experiments that can be performed during a single mission as well as transporting supplies to support different types of missions. This would enable humanity to learn more about its immediate surroundings: the solar system. And in turn, might be able to gain more knowledge about the origins of the universe. The HIAD technology has the potential to enable us to increase the scope of our endeavors to learn more about the world that we inhabit. This means that the development of this technology can pay dividends that are more valuable than what it would take to get this technology to work and provide useful benefits. The payload shifting mechanism promises to control the trajectory of the HIAD while decreasing its velocity to a level that is suitable for landing the payload. A hydraulic system is able to provide a suitable response time that would enable the payload shifting mechanism to modulate the L/D ratio and also hold a specific L/D, if desired, for an extended period of time.

Appendix

Appendix A –Engineering Drawings

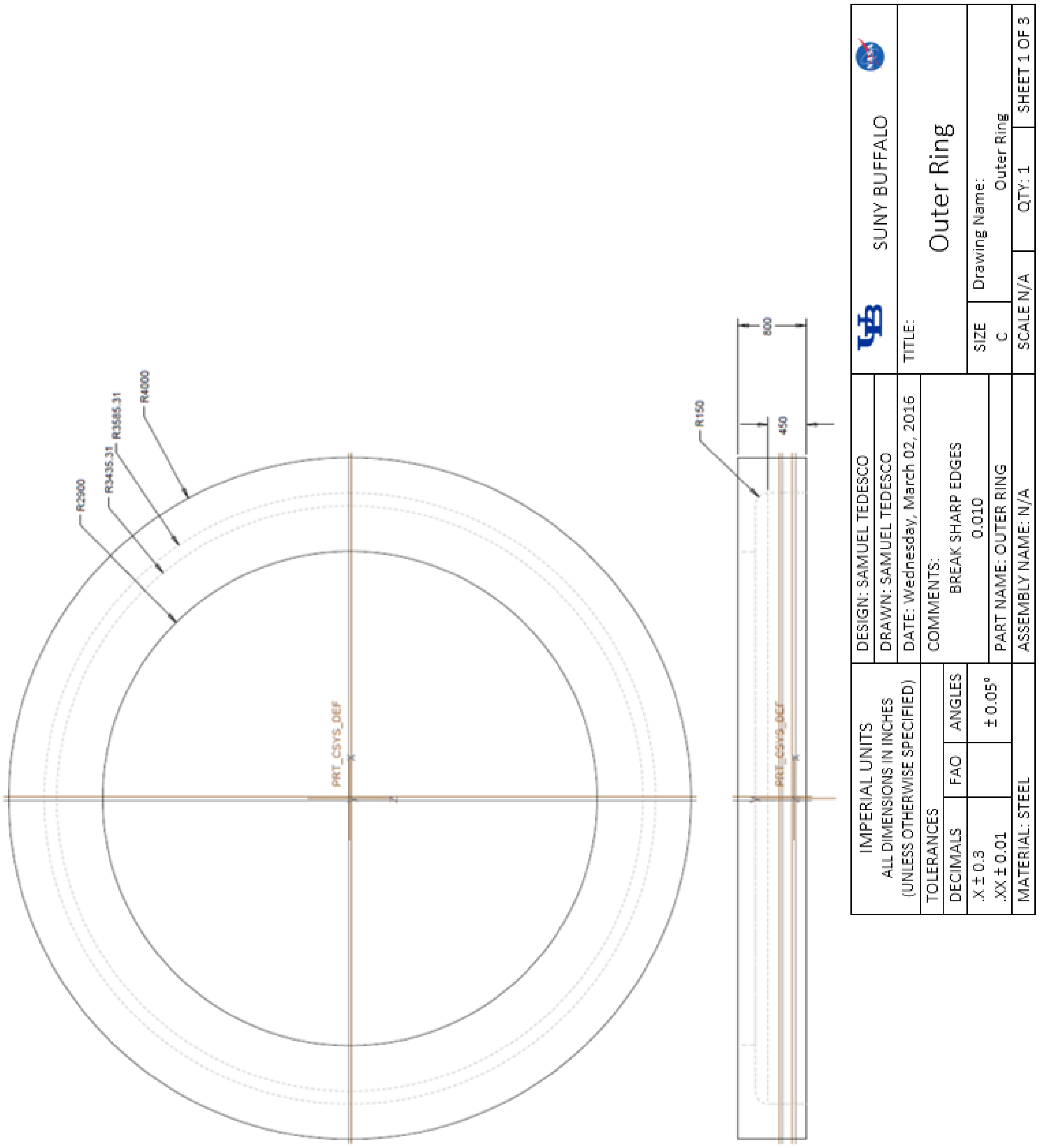

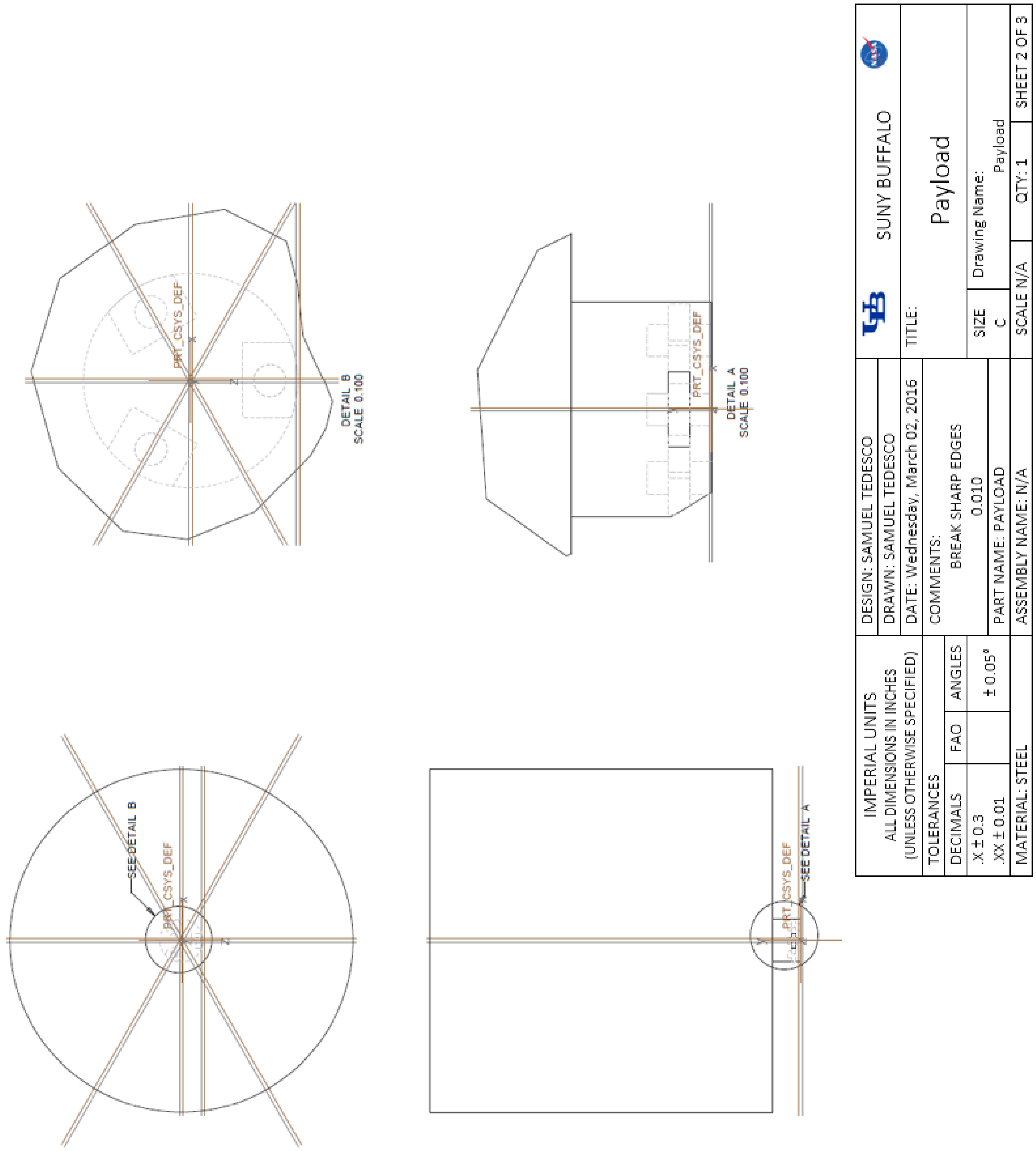
PRT_CSYS_DEF
DETAIL B
SCALE 0.100
DETAIL A
SCALE 0.100
SEE DETAIL B
SEE DETAIL A
IMPERIAL UNITS
ALL DIMENSIONS IN INCHES
(UNLESS OTHERWISE SPECIFIED)
TOLERANCES
DECIMALS
FAO
ANGLES
.X ± 0.3
.XX ± 0.01
± 0.05°
MATERIAL: STEEL
DESIGN: SAMUEL TEDESCO
DRAWN: SAMUEL TEDESCO
DATE: Wednesday, March 02, 2016
COMMENTS:
BREAK SHARP EDGES
0.010
PART NAME: PAYLOAD
ASSEMBLY NAME: N/A
SUNY BUFFALO
TITLE:
Payload
SIZE
C
Drawing Name:
Payload
SCALE N/A
QTY: 1
SHEET 2 OF 3

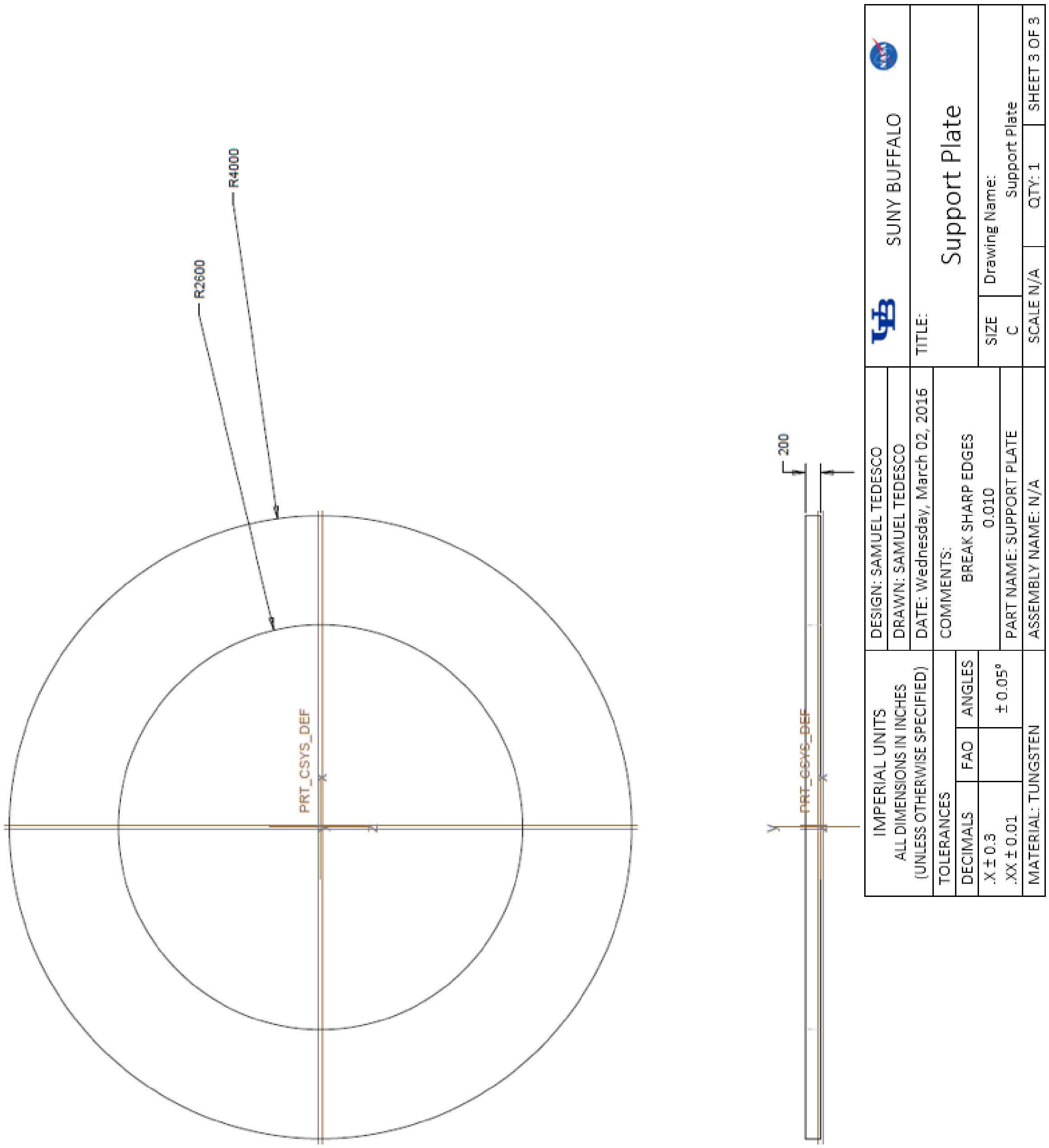
R2600
R4000
PRT_CSYS_DEF
200
PRT_CSYS_DEF
IMPERIAL UNITS
ALL DIMENSIONS IN INCHES
(UNLESS OTHERWISE SPECIFIED)
TOLERANCES
DECIMALS
FAO
ANGLES
.X ± 0.3
.XX ± 0.01
± 0.05°
MATERIAL: TUNGSTEN
DESIGN: SAMUEL TEDESCO
DRAWN: SAMUEL TEDESCO
DATE: Wednesday, March 02, 2016
COMMENTS:
BREAK SHARP EDGES
0.010
PART NAME: SUPPORT PLATE
ASSEMBLY NAME: N/A
SUNY BUFFALO
TITLE:
Support Plate
SIZE
C
Drawing Name:
Support Plate
SCALE N/A
QTY: 1
SHEET 3 OF 3

Appendix B – MATLAB Code

Hypersonic Entry, Oblique Shock

```
clear all
close all
clc

%% Assumed Mars Surface Constants

P = 25 % Pa
T = 218 % K

%% Variables

M = [10.2:-.0337:.07] % Mach number at specified height
H = 50000 % m
T_m = 271.1 - 2.35*H/1000; % Molecular-scale Temperature
y = 0.000001409*T_m^2 - 0.001192*T_m + 1.5175 % specific heat ratio of Mars
L = 20 % m; length of HIAD
Theta = 25 % Half-angle of HIAD conical structure
Theta_a = [10:.1:40] % Angle adjusted to through shifting CG
n = 2 % Shock solution
pi = 3.14 % pi

%%

A = pi*(L/2)^2;
a = [1 + (y - 1)/2*(M.^2)]*tand(Theta);
b = (1 - M.^2);
c = [1 + (y + 1)/2*(M.^2)]*tand(Theta);
lambda = sqrt(b.^2 - 3.*a.*c);
chi = (9.*a.*b.*c - 2.*b.^3 - 27.*a.^2)/(2.*lambda.^3);
beta = atan((-b + 2*lambda*cos(acos(chi)/3 + 2.*pi.*n/3))/(3.*a));
beta2 = beta*180/pi;

M_n1 = M*sind(beta2);
M_n2 = sqrt((1 + (y - 1)/2*(M_n1).^2)/(y*(M_n1).^2 - (y - 1)/2));
M2 = M_n2/(sind(beta2 - Theta));

P2 = P*(1 + 2*y*(M_n1.^2 - 1)/(1 + y));

F = P2*A;

Lift = F.*sind(Theta_a)
Drag = F.*cosd(Theta_a)

Lift_Drag_Ratio = Lift./Drag

plot(Theta_a,Lift_Drag_Ratio);
title('Lift Drag Ratio at Adjustment Angle')
xlabel('Angle Adjusted To')
ylabel('Lift Drag Ratio')
```

Hypersonic Entry, Normal Shock

```
clear all
close all
clc
% Normal Shock

%% Assumed Mars Surface Constants

P = 25 % Pa
T = 218 % K

%% Variables

M = 10.2 % Mach number at specified height
H = 50000 % m
T_m = 271.1 - 2.35*H/1000; % Molecular-scale Temperature
y = 0.000001409*T_m^2 - 0.001192*T_m + 1.5175 % specific heat ratio of Mars
L = 20 % m; length of HIAD
h = 6.428 % m; height of TPS
Theta_a = 25 % Angle adjusted to through shifting CG
pi = 3.14 % pi

%%

P2 = ((2*y)/(y + 1)*M^2 - (y - 1)/(y + 1))*P;

P02 = P2*(((y + 1)/2*M^2)/((2*y/(y + 1))*M^2 - (y - 1)/(y + 1)))^(y/(y-1));

Lift = P02*pi*(L/2)*sind(Theta_a)*((L/2) + sqrt(h^2 + (L/2)^2))

Drag = P02*pi*(L/2)*cosd(Theta_a)*((L/2) + sqrt(h^2 + (L/2)^2))

Lift_Drag_Ratio = Lift/Drag
```

References

[1] *NIA, Breakthrough, Innovative, Game-changing (BIG) Idea Challenge* Web. 1 Oct. 2015. <http://www.bigidea.nianet.org/>.

[2] Marraffa, L. "CESMA 001 14 Hypersonic Technologies and Atmospheric Entry Missions at ESA, L. Marraffa, ESA/ESTEC." YouTube. YouTube, 19 July 2014. Web. 1 Nov. 2015.

[3] Hansen, James R. (Jun 1987). "Chapter 12: Hypersonics and the Transition to Space". *Engineer in Charge: A History of the Langley Aeronautical Laboratory, 1917-1958*. The NASA History Series. sp-4305. United States Government Printing. ISBN 978-0-318-23455-7.

[4] Williams, David R. "Mars Fact Sheet." Mars Fact Sheet. NASA Goddard Space Flight Center, 29 Feb. 2012. Web. 05 Mar. 2016. <http://nssdc.gsfc.nasa.gov/planetary/factsheet/marsfact.html>.

[5] Arnett, Bill. "Mars." Nine Planets. 21 Aug. 2009. Web. 27 Nov. 2009. <http://www.nineplanets.org/mars.html>.

[6] Barry, Patrick. "NASA Mission to Study the Moon's Fragile Atmosphere." NASA. NASA, 23 Oct. 2009. Web. 28 Nov. 2009. <http://science.nasa.gov/headlines/y2...3oct_ladee.htm>.

[7] Coffey, Jerry. "Atmosphere of Mars - Universe Today." Universe Today. Universe Today, 19 Dec. 2008. Web. http://www.universetoday.com/22587/atmosphere-of-mars/

[8] Enerpac. "BRC, BRP-Series, Pull Cylinders." Pull Cylinders, Single Acting: BRC, BHP Series. Enerpac, 25 Jan. 2013. Web. <http://www.enerpac.com/en-us/industrial-tools-imperial/hydraulic-cylinders-jacks-lifting-products-and-systems/general-purpose-hydraulic-cylinders/brc-brp-series-pull-cylinders>.

[9] Potter USA. "20 Ton Hydraulic Cylinder." Potter USA. Potter USA, 16 Nov. 2015. Web. <http://www.potterusa.com/electric-hydraulic-cylinders/762-20-ton-hydraulic-cylinder-.html>.

[10] Grainger. "Electric Hydraulic Pumps." Grainger Tools. Grainger, 05 Mar. 2015. Web. <https://www.grainger.com/category/electric-hydraulic-pumps/pumps/hydraulics/ecatalog/N-pil?ssf=3#nav=%2Fcategory%2Felectric-hydraulic-pumps%2Fpumps%2Fhydraulics%2Fecatalog%2FN-pilZ1yzp5xv%3Fssf%3D3>.

[11] Vector Mechanics for Engineers, Statics & Dynamics, 3rd Ed.; F. P. Beer & E. R. Johnston Jr., McGraw-Hill, 1977.

[12] Fundamentals of Physics, Davis Halliday & Robert Resnick, John Wiley & Sons Inc., 1974.

[13] Fundamentals of Classical Thermodynamics, 2nd Ed.; G. J. VanWylen & R. E. Sonntag, John Wiley & Sons, 1978.

[14] Planetary Atmospheres / Venus, P. J. Gierasch, Cornell University & Y. L. Yung, California Institute of Technology, 2003

[15] Stevens, Chris. "Industrial Metals Prices and Charts - Data from Quandl." Industrial Metals Prices and Charts - Data from Quandl. Quandl, 05 Mar. 2016. Web. 05 Mar. 2016. <https://www.quandl.com/collections/markets/industrial-metals>.